ANTAL KERPELY DOCTORAL SCHOOL OF MATERIALS SCIENCE & TECHNOLOGY

Phenomena upon Brazing of Steels by Copper

A PhD dissertation submitted to Antal Kerpely Doctoral School for the degree of

Doctor of Philosophy in the subject of Material Science and Technology

By

Dheeraj Varanasi

Supervisors

Dr. Peter Baumli, Associate Professor

Prof. George Kaptay, Professor

Head of the Doctoral School

Prof. Gacsi Zoltan

Institute of Metallurgy, Metal Forming and Nanotechnology

Faculty of Material Science and Engineering

University of Miskolc, Hungary

November 2020

1. Introduction

Steels are the most commonly used structural materials owing to their superior properties like strength, ductility, rigidity etc. Brazing is a type of thermo-mechanical joining technology where a third material is melted between the two substrates to be joined in order to achieve a permanent joint. It is usually carried out in controlled environments at temperatures above 723 K. The cohesion between substrates and braze filler play a crucial role in determining the joint properties [1,2]. More often than not, Cu is the widely used braze metal as it is cheaper and cost-effective and is still the common practice in the industry. Thus, steels and copper are the two most important materials from industrial point of view and hence an in depth understanding of the various phenomena occurring during brazing of two most important materials is quite necessary. This thesis is a genuine effort in investigating the various phenomena accompanying the process of brazing.

2. Summary of Literature

This section is focused on presenting the identified knowledge gaps in the literature concerning the various phenomena observed during a brazing process.

2.1 The role of the oxide layer in brazing

Brazing experiments are usually carried out under three environments – oxidizing environment (carried under air pressure), reducing environment (under H_2 or CO environment) and inert environments (under Ar / N_2 gas or vacuum) [3]. Controlled environments are helpful in controlling the surface contaminants like oxides which will result in poor wetting of the liquid metal and solid surface. Hence, removal of oxide layer is very important for brazing process. Reports on oxide removal from the surface of stainless steels under vacuum at residual pressures between E-5 and E-8 bar at temperatures between 1123 … 1273 K were carried out previously [4-6]. These steels are high in Cr and Ni. Similar study reported by Rosseau2016 [7] under N_2 environment at 2 bar, found oxide removal temperature of 1073 K from surface of high speed steels (Cr-V-Mo-C).

Knowledge gap: We notice that although there are many papers in the literature that studied the conditions of the removal of the oxide layer from the surface of steels, these studies are focused only on limited range of steels (stainless steels or high-speed steels) and mostly under inert or oxidizing environments. A systematic study is missing on the other steels such as carbon steels or low-alloy steels. The effect of engineering parameters of pressure and composition of steels on the dissociation temperature of oxide needs to be investigated.

2.2 Wetting of steels by liquid metals

Wetting according to Hawkins et al. [8] is the spread of liquid on top of a solid surface which continues until the surface energies are balanced, according to Eq. (1) [9].

$$cos\theta = \frac{\sigma_{sv}-\sigma_{sl}}{\sigma_{lv}} \quad (1)$$

where σ_{sv} (J/m^2) is the solid-vapor interface energy, σ_{sl} (J/m^2) is the solid-liquid interface energy and σ_{lv} (J/m^2) is the surface tension of the liquid (liquid-vapor), θ (degrees) is the contact angle between the droplet edge and solid surface at the triple point.

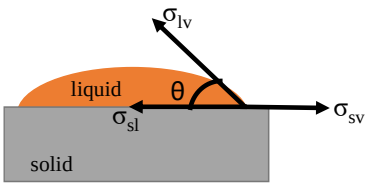

Fig.2.2-1. Illustration of sessile drop wetting technique, most commonly used method for determining the wettability of solid-liquid systems

The contact angles of metallic liquids like Cu, Ag, Au on their own solids were found in the range of 0 to 10°, excellent metal/metal wetting [10-11]. For the molten liquids involved in the study such as Sn and Cu, the wetting angles on the surface of Fe are found in literature for Sn/Fe at 1023 K as around 40° albeit under H_2 gas environment [12]. For liquid Cu/steel the contact angle at 1373 K was found to be ~5° under flux environment [13].

Knowledge gap: Although, literature on wetting of steels by liquid tin and liquid Cu exists, the studies were limited to either pure iron or only certain steel types. The information pertaining to liquid metal interactions (Sn, Cu) with other steel types such as medium carbon steels, low alloyed steels, tool steels etc is missing. The information on these interactions should also be investigated as function of various environmental and experimental parameters (temperature, pressure).

2.3 Grain boundary wetting and penetration

Grain boundary is defined as the separation between two adjacent grains in a metal differing in orientation, composition or dimension of crystal lattice [14-15]. The inherent condition for penetration of a solid GB by a molten metal is given in Eq. (2), [16-17].

$$cos\left(\frac{\varphi}{2}\right) = \frac{\sigma_{GB}}{2\sigma_{sl}} \tag{2}$$

Where, σ_{GB} (J/m^2) and σ_{sl} (J/m^2) are the grain boundary energy and solid/liquid interface energy respectively, φ is the dihedral angle and is defined as angle between the liquid layer and the intersecting solid GB, see Fig.2.3-1. GB penetration occurs only when dihedral angle φ is 0° and is considered as measure of penetrability.

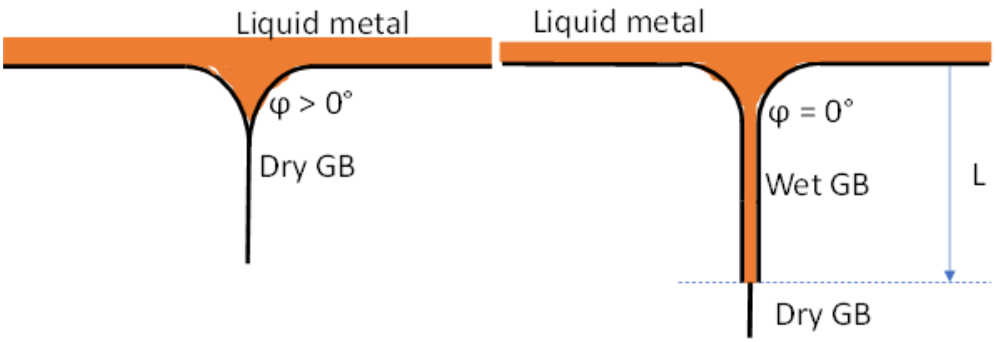

Fig.2.3-1. Schematic of grain boundary penetration by liquid metal showing both dry and wet GB, corresponding dihedral angles and GB penetration depth.

Interactions between Steel and liquid tin were reported by [18-19]. Interactions of Fe, steel with liquid copper with onus on wetting and penetration by liquid copper [20-21]. Penetration depth usually follows from Fick's laws of diffusion and has proportionality of $t^{0.5}$ with time. Fredriksson furthermore found the depth of penetration to vary as function of $t^{0.75}$ [21].

Knowledge gap: Though the literature exists on steel/Cu interactions with regards to grain boundary wetting and grain boundary penetration, the extent of these studies was only limited to high alloyed stainless steels. Data pertaining to the same is insufficient for other structural and carbon steels. Grain boundary wetting and penetration was not extensively studied with respect to the composition of various steels.

2.4 Thinning of the braze joint

Significance of thickness of braze joint comes from the significance of joint gap in brazing process. Normally for brazing application under air, a limit of 0.05 mm joint gap exists for production of good joints establishing the relation - the narrower the gap maintained, better is the quality of the joint [3].

Knowledge gap: From literature, it is discussed that for good joints thinner joint thickness is desirable. It is not known how the joint thickness depends on different brazing parameters, such as brazing time, temperature, steel composition, brazing atmosphere, etc. However, in my study I noticed a reduction in the thickness of the joint which was not reported previously.

2.5 Cracking of the braze joint upon cooling

Once, aforementioned parameters of brazing are satisfied, the focus shifts to the qualitative analysis of the brazed joints – microstructure. Cracks in the joints will cause hindrance to the joint life and serviceability of the brazed structures and hence is an important aspect of brazing. Cracking under external loading was studied extensively in literature under liquid metal embrittlement (LME) which occurs during the mechanical testing of brazed joints [22-23]. Cracking of the brazed joints due to formation of precipitates in the braze joint were carried out by Maciejewski et al. and Ghovanlou et al. [24-25]. In particular brazed steel joints by copper showed joint failure due to manganese sulfide (MnS) precipitation as purported by Ghovanlou et al. [25] is very important from point of view of this study. During processing of steels, ionic precipitates like MnS would be formed was already reported in literature [26].

Knowledge gap: Literature regarding the cracking of brazing joints has been studied before, it focusses on cracking of the joint under external loading conditions. No real contribution was made in the study of cracking of brazed joints under no-load conditions. The gap exists in understanding the cracking of an unloaded joint as function of composition of steels and time. Also, conclusive proof is missing on whether MnS is in fact connected with the cracked braze joints. There is a requirement of a databank on the quality of brazed joints obtained as function of holding time, composition of steels and temperature.

3. Scientific goals

After careful literature review and identification of knowledge gap, the following scientific goals have been defined:

3.1 Identify the conditions of spontaneous removal of the oxide layer from the surface of steels.

3.2 Investigate the wetting behavior of liquid copper and liquid tin on the surface of various steels.

3.3 To investigate the grain boundary penetration of steels by molten copper and molten tin.

3.4 Observe the change in the thickness of the joint and establish the relation between the thickness of the joint and liquid time for various steel compositions.

3.5 Braze of steels by copper and qualitative investigation of the microstructure of the joint. Establishing conditions of spontaneous cracking of the joint upon cooling after brazing, if any.

4. Materials and methods

All the experiments with regards to oxide layer dissociation, wetting, GB penetration and brazing were conducted with following different steels of varying composition. The composition of these steels was tabulated below, Table C1 in claims section.

Pure copper foil [99.99 w%, source: XRD] was used as the braze filler for brazing experiments. The thickness of the copper was 70micrometers, measured by using micrometer. Pure tin [99.99w%, source: XRD] and pure copper were used to study the oxide layer removal and wetting experiments. The experiments were conducted in a resistance vacuum furnace equipped with Pt/Pt-Rh thermocouple to measure the temperature. All the steel samples were first cut to required dimensions of 10mm · 7mm · 4mm and ground by using sand papers of 180, 220 and 320 µm grit size and to polishing on a 3µm grit woolen cloth in a diamond media using alumina paste and dried immediately. Both grinding and polishing are carried out at 25N load at 300 rpm speed of the disc. To study the oxide layer dissociation/removal and corresponding wetting, a sessile drop technique is used [27], refer Fig.C1 in claims section. For the purpose of brazing, the two steels and Cu foil are placed in a sandwich structure where the foil is in between the two steels, high temperature wire is wound around the sandwich structure so as to keep them in place during the experimentation, refer Fig.C2 in claims section. Post experimentation, the samples were left to cool overnight, later removed from furnace, weighed, mounted in resin for microstructural examination. Scanning electron microscopy (SEM) is used for microstructural examination. Two different scanning electron microscopes were used in this study, Carl Zeiss EVO MA10 and Hitachi S-4800. EDAX Genesis APEX2 and Bruker AXS EDS were used for carrying the elemental analysis at the microstructure. An acceleration voltage of 20KV was used. All the pictures were taken under back scattered scanning electron microscopy (BSD-SEM) mode. ImageJ software is used for image analysis.

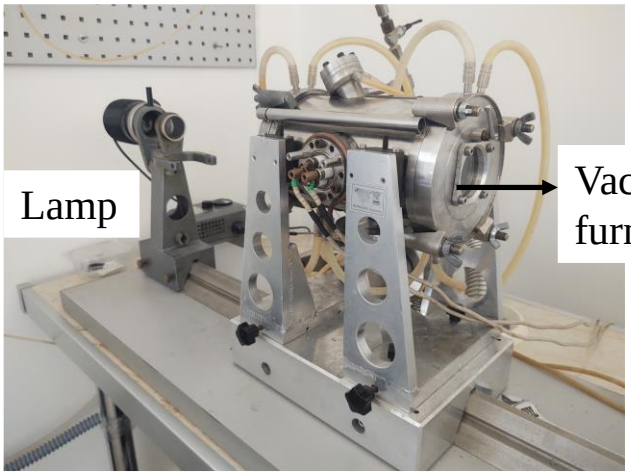

Fig.4.1. The furnace used for the experiments

5. Results

5.1. The role of the oxide layer in brazing and wetting of steels by liquid tin

From the literature, it was clear that the steel surfaces are covered by a native oxide layer which hinders wetting of solids by liquid metals. The experiments were focused on observing the conditions under which the native oxide layer disappears during wetting. Liquid tin was used as the molten metal as it has broad liquid temperature range. The experiments were conducted at two different residual pressures in vacuum E-5 bar and 9E-8 bar to observe if pressure has any significant difference. The range of temperature for all the steels was in between 673-1273 K.

After the wetting transition of liquid tin on the surface of steels, wetting of steel surfaces by molten tin follows. Spreading of liquid tin occurs after non-wetting to wetting transition. The contact angles between liquid tin and steel surface were measured continuously using the KSV surface analysis software. SEM investigations also revealed formation of Fe/Sn intermetallic layers at the steel/tin interface. Find the results pertaining to this section in claims section 6.1.

5.2. Wetting of steel surfaces by liquid copper

The melting point of copper (1358 K) and the experimental brazing temperature (1373 K). Hence in the wetting experiments with copper, by the time copper melts, an instantaneous wetting and spreading was observed with contact angles < 10° showing a near perfect wetting between molten copper and steels. Find the experimental results concerning with this section in claims 6.2. The experimental results are in agreement with theoretical analysis as shown in section 6.2

5.3. Grain boundary wetting and penetration of steels by liquid metals

5.3.1. Grain boundary wetting and penetration of steels by liquid tin

Grain boundary wetting and grain boundary penetration are undesirable phenomena. No grain boundary penetration by liquid tin was observed in Armco, C45, S103 and CK60 steels which is a consequence of formation of continuous intermetallic layer that closes the steel grain

boundary for liquid tin to access maintaining the dihedral angle φ > 0. However, GB penetration was observed by liquid tin into the EN1.4034 steel grain boundary and a dihedral angle φ = 0° which is attributed to the high Cr-composition of this steel [28, 29]. The results were discussed in section 6.3b.

5.3.2. Grain boundary wetting and penetration of steels by liquid copper

GB wetting between steel/Cu is accompanied by dissolution of Fe from the bulk steel in liquid copper during experiment. GB penetration was observed in all the steel/Cu systems with dihedral angle, ϕ = 0°. However, the depth of penetration varied depending on the alloying composition of the steel. we observe an average depth of penetration between 10 to 20 µm is achieved by liquid copper in the five different steels under experimental conditions.

5.4. Rapid thinning of the brazed joint

Before arranging the samples in a sandwich structure Fig.C2, the surface roughness of the steels was measured. Measured average surface roughness of steel surfaces was between 0.015 to 0.030 µm.

The initial thickness of braze foil is 70µm which should be the joint thickness in ideal case. However, reduction in thickness of Cu joint (d_j) was observed which reduced rapidly with liquid time, (t_L, s). Liquid time is defined as the time duration for which the sample was in the temperature range between 1356 … 1373 K. This equals the entire duration of the holding time at 1373 K + time interval during heating + the time interval of 1373 K … 1364 K during cooling, Fig.5.4-1. Here, T = 1364 K is obtained as average between holding temperature (1373 K) and melting point of pure Cu (1356 K). This is because during the holding time liquid Cu becomes saturated by Fe and Fe-Cu system is peritectic, solidifying in the T-range of 1373 … 1356 K. The relation between t_h and t_L was formulated in Eq. (3), see Fig.5.4-2.

$$t_L = t_h + 68 \tag{3}$$

Where, t_L (s) and t_h (s) are the liquid time and holding time respectively.

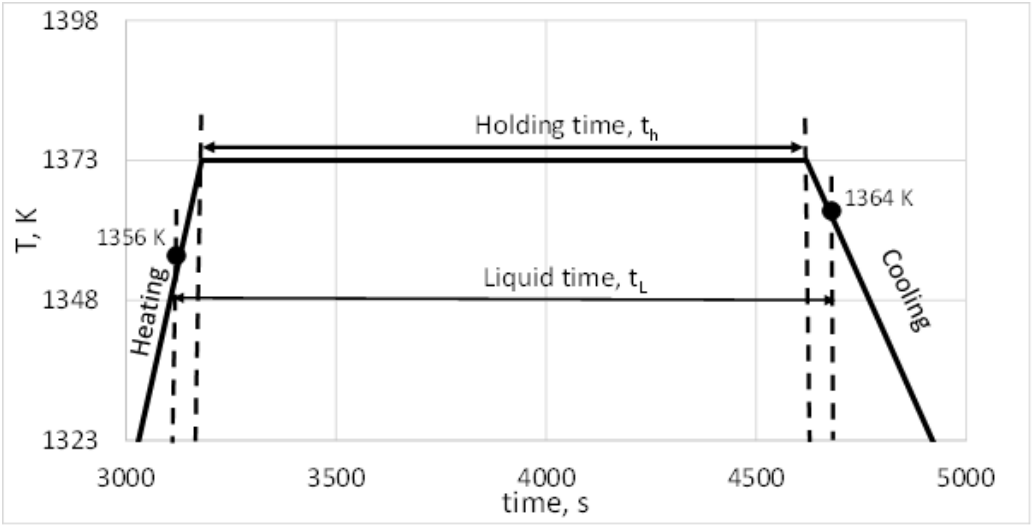

Fig.5.4-1. Schematic showing the relationship between holding time t_h and liquid time t_L

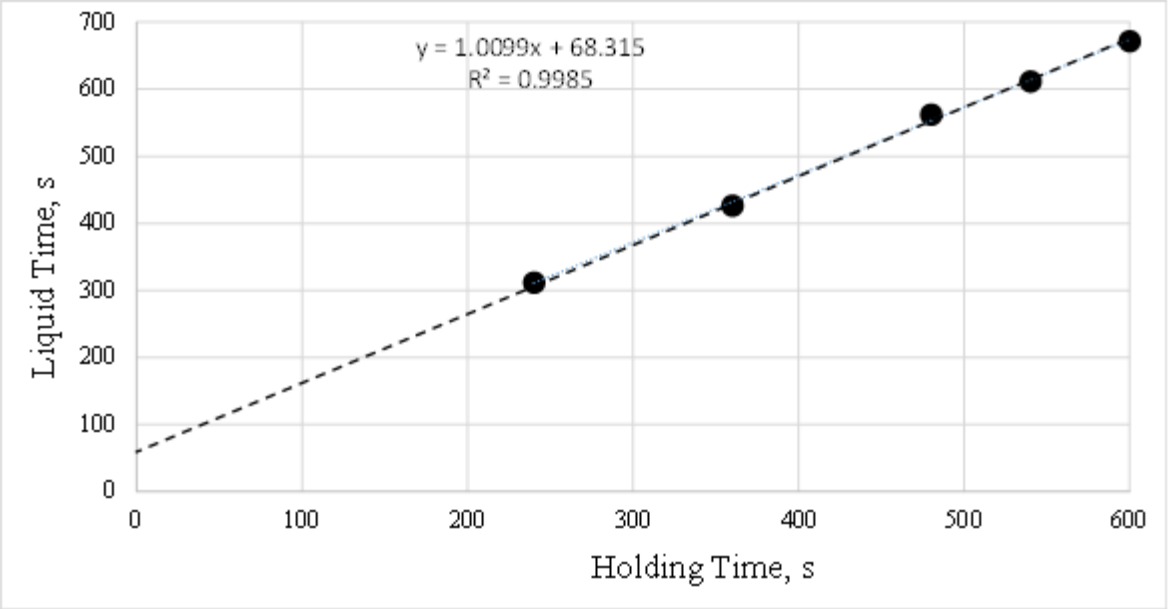

Fig.5.4-2. The relation between the liquid time and holding time during the brazing experiments.

The reduction of thickness of the brazed joint across all the experiments was observed as function of liquid time and composition of steel by a varying parameter, "z, semi-empirical reduction coefficient". Find the results in section 6.4

5.5. Cracking of the braze joint upon cooling

5.5.1. Observation of cracking in the brazed joints

Spontaneous cracking of the brazed joints under no load conditions was observed in steels as function of composition of Mn and S in the steels. No cracking was observed for low alloyed C45 and Armco steels with low Mn and S concentration at 1884 s liquid time (at least). While for other steels with increasing Mn and S concentrations (S103, CK60 and EN1.4034 steels) spontaneous cracking was observed in the joints after a certain critical liquid time. The critical liquid time required for cracking was decreased as the concentration of Mn and S increased in the steels. The prime reason for cracking of the brazed joints was found to be the MnS precipitates in the joint upon cooling. Find the results and discussion on these experiments and cracking of the braze joints in the section 6.5 (a-c).

6. Claims

All claims are based on the series of experiments conducted with a 70-micron thick pure copper foil placed in between two identical steel plates, Table C1, dimensions 10mm · 7mm · 5mm to form a sandwich structure as shown in Fig.C1. The sandwich is wound tightly by a high temperature wire to keep them in place during the experiments. The sandwich then is placed inside a resistance heating vacuum furnace. The experiments are conducted at a temperature of 1373 K at a residual pressure of around 10^{-8} bar (or in some cases at around 10^{-5} bar). The heating rate of the furnace is around 293 k/min and the temperature inside the furnace is measured by a Pt-Pt-Rh thermocouple. After given holding time at 1373 K the furnace is cooled

down spontaneously overnight (keeping the vacuum) and the sample is removed the next morning.

Table C1. The composition of the various steels used in this study

Steel standard		Cr wt%	Mn wt%	S wt%	C wt%	Others (Si, P, Mo etc) wt%	Fe wt%
European	AISI						
Armco	-	0.016	0.11	0.0064	0.0010	< 0.050	Rest
C45	1045	-	-	0.030	0.45-0.50	~ 0.60	Rest
S103	-	-	0.20-0.25	0.010-0.020	0.60-1.00	~ 0.70	Rest
CK60	1060	0.15-0.20	0.75-0.80	0.070-0.075	0.25-0.60	~ 0.70	Rest
EN 1.4034	420	11-12	0.90-1.0	0.035	0.15-0.20	~ 0.50	Rest

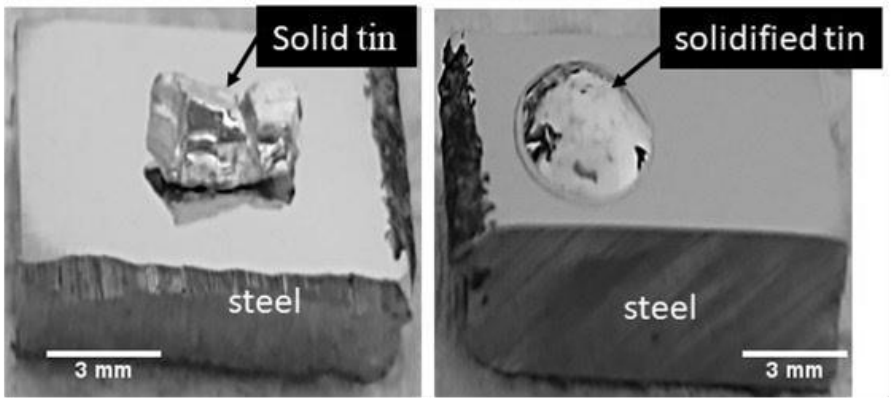

Fig.C1. The tin on surface of steel, pre and post wetting experiments. Solid tin piece is seen in the left side picture before wetting experimentation. Sessile drop of tin is seen in the right-side picture indicating the melting and solidification of tin on the surface of steel.

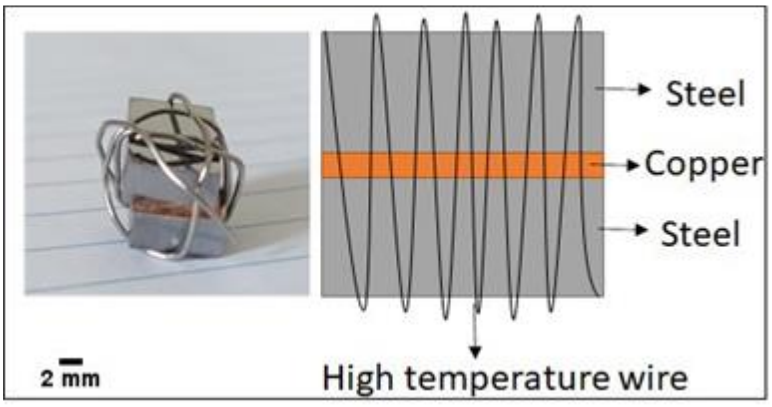

Fig.C2. The sandwich arrangement of the copper foil and steel plates used throughout the study

Though the experiments were conducted during given "holding time" at 1373 K, for consistency and generalization "liquid time" was used in the claims. Liquid time here is defined as time of the braze under liquid state (time maintained above the melting point of pure copper

= 1356 K) during the given experiment. It includes the entire duration of holding time of the experiment plus part of the heating time and part of the cooling time as explained in section 5.4. The empirical relationship between the liquid time and holding time in our furnace was found as:

$$t_L = t_h + 68 \quad \text{(C1)}$$

where t_L is liquid time (s), t_h is holding time (s). As each furnace is different, Eq. (C1) is different for each furnace. That is why the claims in this thesis are formulated as function of liquid time, so the claims have general validity for any furnace.

The claims below are formulated according to the sequence of different phenomena that take place during brazing process.

6.1. Spontaneous removal of the native oxide layer from the surface of steels

The removal of the native oxide layer from the surface of steels was observed experimentally measuring the change from the non-wetting to wetting states of liquid tin on the surface of steels. The critical temperature of oxide removal on different steels at two different residual pressures of vacuum was tabulated in Table C2. Successful brazing of different steel types at given vacuum levels are possible only above the transition temperatures given in Table C2.

Table C2. Wetting transition temperatures of liquid tin on various steels

Steel	Transition temperature (K) at 10^{-8} bar vacuum	Transition temperature (K) at 10^{-5} bar vacuum
Armco	773-793	773-793
C45	823-843	823-843
S103	913-933	963-983
CK60	923-943	973-993
EN1.4034	1133-1153	No transition below 1273 K

Liquid tin transition experiments from claim 1 show that the oxide layer is removed and the liquid tin has transitioned successfully from non-wetting to wetting liquid on the surface of steels, (see Fig.C3 and Table C3). The relatively high contact angles shown in Table C3 as compared to liquid copper/steel system are due to the formation of not-fully metallic intermetallic compounds at the steel/Sn interface, (see Fig.C4).

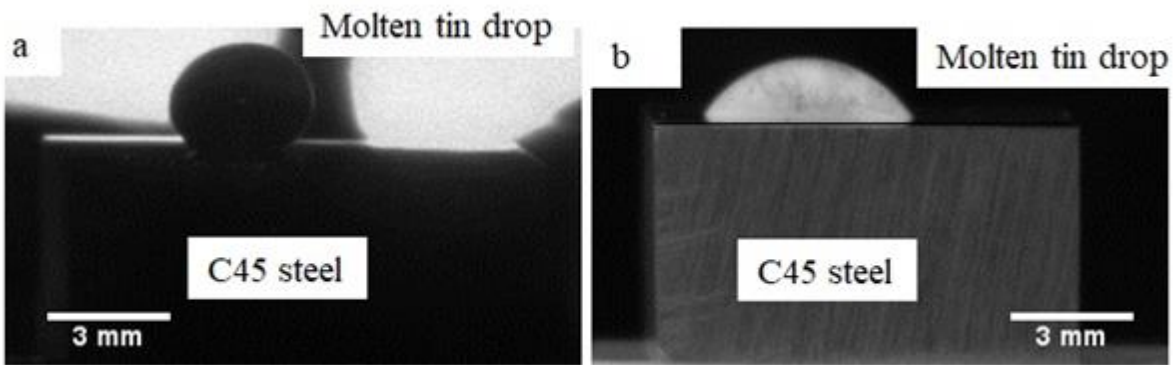

Fig.C3. Transition of liquid tin drop from non-wetting at 573 K (a) to wetting at 933 K (b) on the surface of C45 steel, at 10^{-8} bar residual pressure.

Table C3. final contact angles of liquid tin on the surface of steels at two different residual vacuum pressures

Steel	10^{-5} bar vacuum pressure		10^{-8} bar vacuum pressure	
	T, K	θ, (°)	T, K	θ, (°)
Armco steel	883	50 ± 10	923	50 ± 10
C45 steel	943	70 ± 10	933	45 ± 10
S103 steel	1033	75 ± 10	973	50 ± 10
CK60 steel	1073	70 ± 10	973	70 ± 10
EN1.4034 steel	1323	130 ± 10	1223	20 ± 10

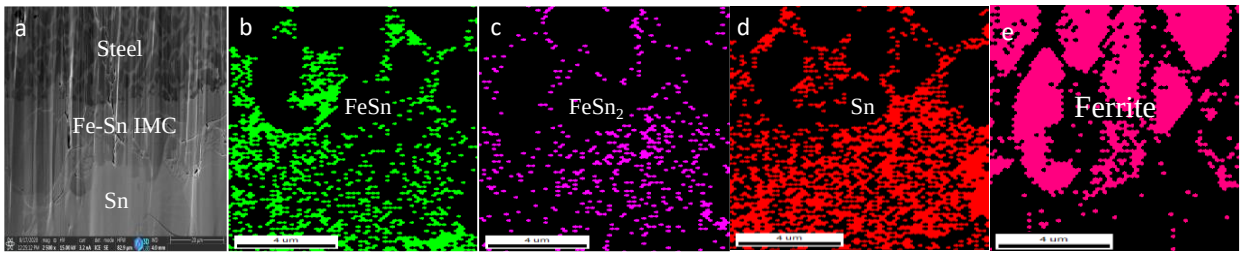

Fig.C4. Formation of Fe/Sn intermetallic compounds at the interface of steel and liquid tin limiting the spreading and wetting of steels by liquid tin.

6.2. Wetting steel surfaces by liquid copper

Thanks to Claim 1, liquid copper was found spreading instantaneously (with near zero contact angle) along the surfaces of all steels at its melting (1356 K) point at 10^{-8} bar vacuum, which is the precondition to form strong joints, (see Fig.C5 and Table C4). The experimentally observed contact angle values were approximately confirmed by the theoretical calculations [30] providing the possible range of contact angles for the Fe/Cu systems between 0° and 20°.

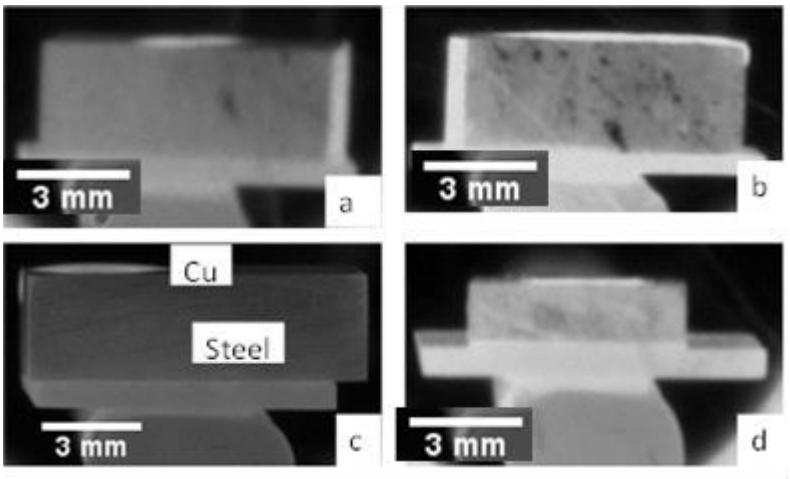

Fig.C5. Close-to-perfect wetting of the copper on various steels observed during the wetting experiments. a: C45 steel, b: S103 steel c: CK60 steel and d: EN1.4034 steel.

Table C4. Final wetting angles of liquid Cu on the surface of various steels

Steel	contact angle of Cu on steel (°)
C45	2.7 ± 0.2
S103	1.3 ± 0.2
CK60	2.4 ± 0.3
EN1.4034	5.0 ± 0.5

6.3. Grain boundary penetration of liquid metals into GB-s of different steels

6.3a. GB penetration by liquid copper

Grain boundary penetration of steels by liquid copper was observed for all the steels studied here. However, the depth of penetration varied as function of composition of steels (see Fig.C6). Average penetration depth of around 10-20 μm was achieved by liquid copper in steel GB's at 300 s holding time.

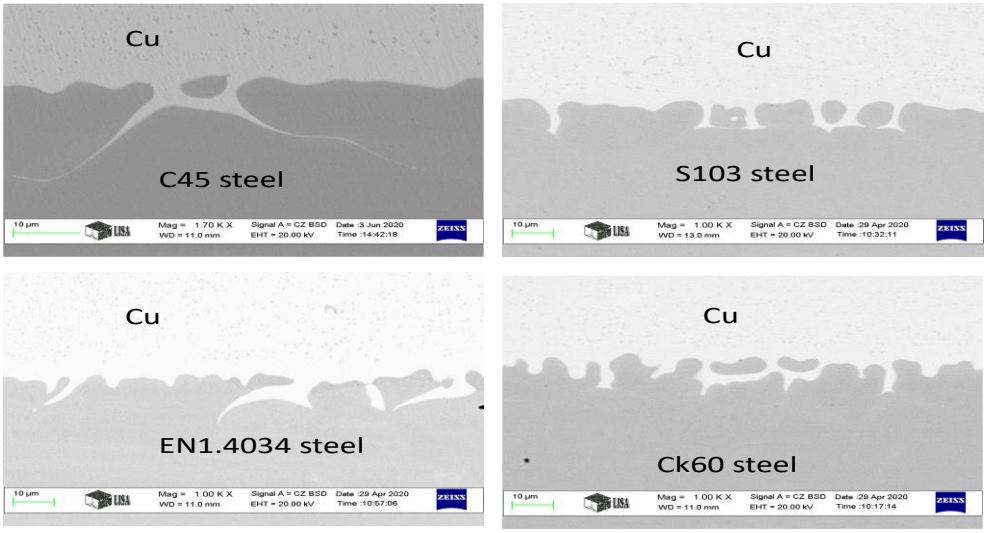

Fig.C6. Grain boundary penetration of steels by liquid copper at 384 s of liquid time.

6.3b. GB penetration by liquid tin

GB penetration was not found by liquid tin in the following four steel types: Armco, C45, S103 and CK60. This can be explained by the formation of continuous Fe/Sn intermetallic layer at the steel/tin interface, blocking the GB-s of steel, so liquid tin cannot penetrate into those GB-s (see Fig.C8). GB penetration was observed only in case of EN1.4034 steel due to its high Cr-content. This leads to liquid metal embrittlement of EN1.4034 steel by liquid tin. The average depth of penetration achieved by liquid tin in this steel was 25 ± 3 μm, at temperature between 1150-1250 K and 600 s holding time (Fig.C7e).

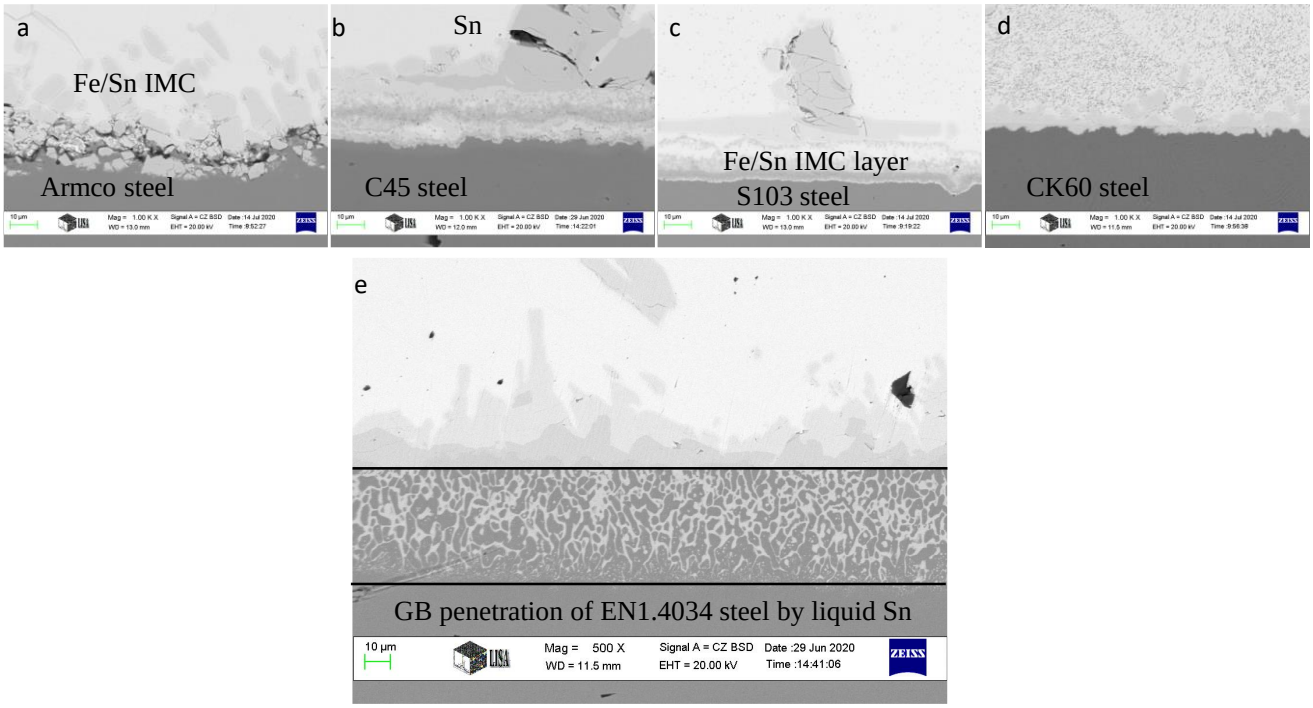

Fig.C7. No GB penetration of four steels by liquid tin seen in Fig-s. a-d. However, GB penetration of liquid tin in EN1.4034 steel (Fig.C8e) can be seen.

6.4. Rapid thinning of the joint after melting

After melting the copper foil, the joint thickness was found to decrease rapidly from its initial thickness of 70 μm as function of liquid time across all the experiments (see Fig.C8). The following general equation was found to describe the liquid time dependence of the thickness of the joint d_j, Eq. (C2):

$$d_j \cong \frac{70}{1+z \cdot t_L} \tag{C2}$$

where d_j (micron) is the thickness of the joint obtained post experimentation, t_L (s) is the liquid time for the experiment, 70 microns is the initial thickness of the Cu foil, while z (1/s) is the semi-empirical coefficient (see Table C5 for its values). As the copper melts, liquid copper is pushed out from between the steels due to the spring force from the wound wire and gravity force from the upper plate. This out pushed copper evaporates as the equilibrium vapor pressure

of copper is 7.94 E-7 bar, being higher than 9 E-8 bar of residual pressure of vacuum inside the furnace.

Table C5. Semi-empirical coefficient for different steel grades to be used in Eq. (C2)

Steel grade	Semi-empirical coefficient, z (1/s)
C45	0.0054 ± 0.001
EN1.4034 and S103	0.017 ± 0.003
CK60	0.045 ± 0.03

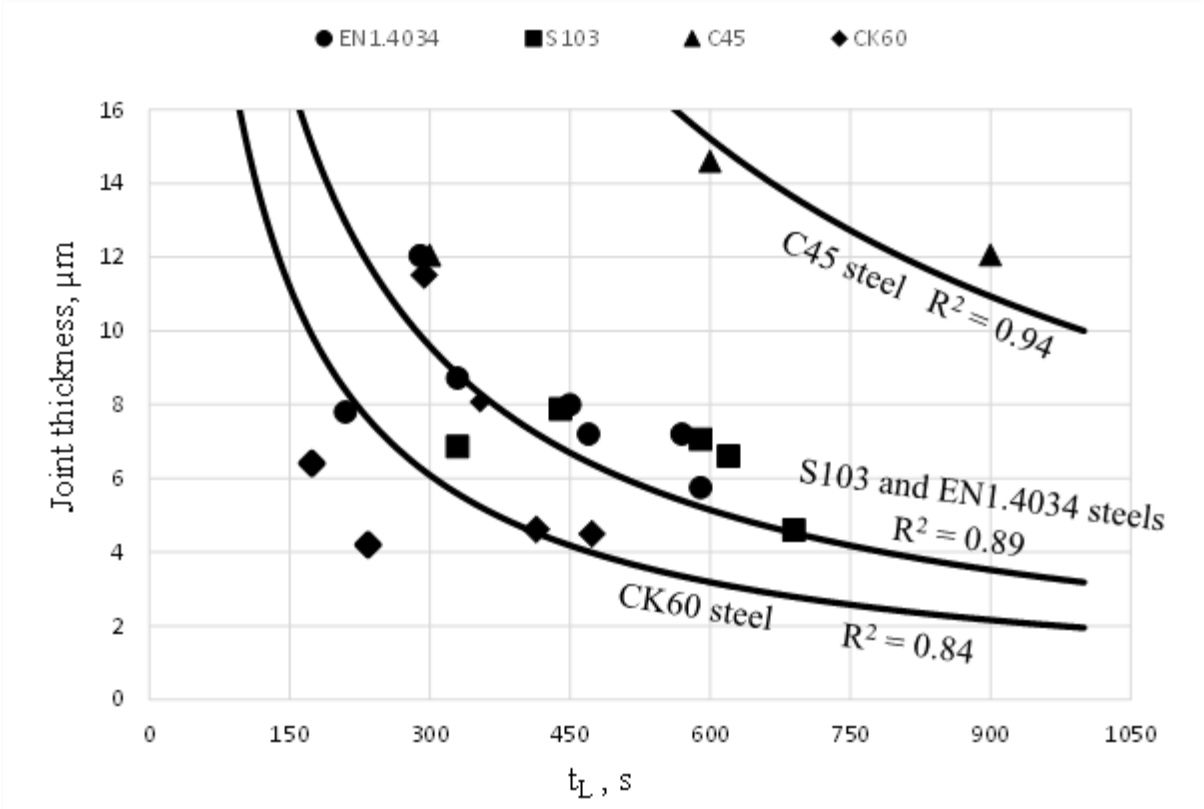

Fig.C8. Variation of the joint thickness between the steel samples as function of the liquid time for various steel types. The three average lines obtained for steel types as indicated in figure by substituting different z values from Table C5 into Eq. (C2).

6.5. Cracking in the unloaded brazed joint upon cooling

6.5a. Cracking observed

No cracking was observed in C45 and Armco steels with experiments after 1868 s liquid time, i.e. the joints were free of any ionic precipitates. However, experiments with steels containing larger amounts of alloying elements (S103, CK60 and EN1.4034) show cracking after a certain liquid time (see Fig.C9). Table C6 shows the minimum liquid time t_L required for cracking the copper brazed joints as function of composition of steels.

Table C6. Mn-S composition in the steel and minimum liquid time needed for cracking the brazed joints

Steel	Mn wt%	S wt%	Liquid time required for cracking of the joint (s)
C45	-	0.03	no cracking up to 1868 s at least
Armco	0.11	0.0064	no cracking up to 1868 s at least
S103	0.25	0.02	578 ± 30
CK60	0.75	0.07	308 ± 30
EN1.4034	1	0.035	338 ± 30

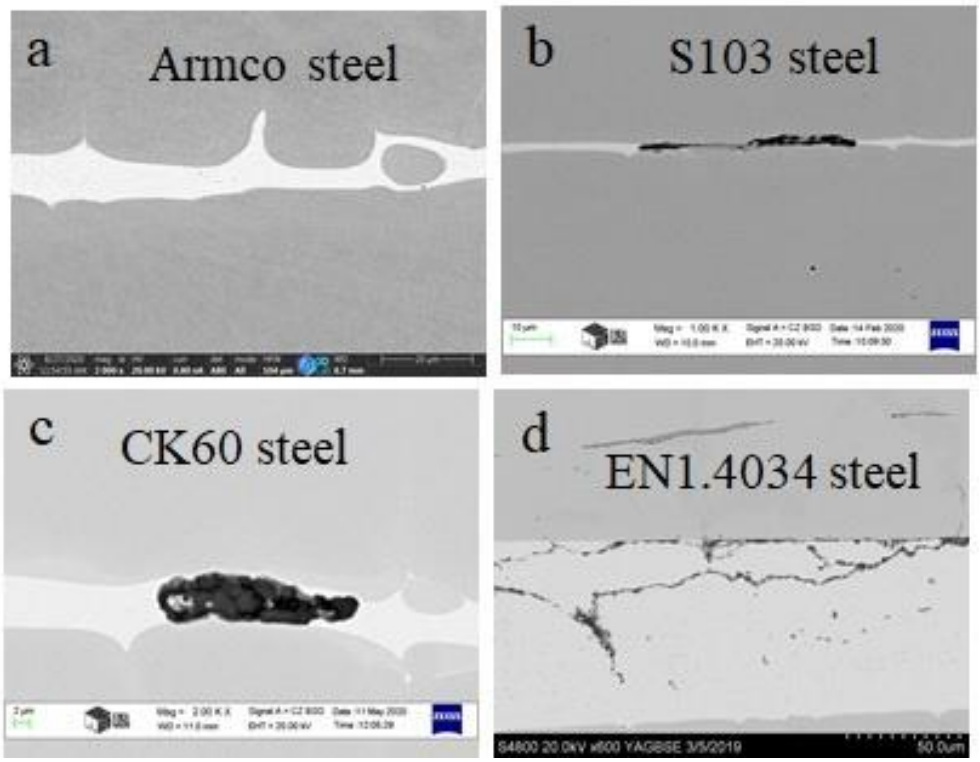

Fig.C9. SEM micrographs of the joints observed in unloaded brazed steel/Cu/steel joints. An uncracked joint is observed for Armco steel, while cracked joints were obtained for other three steels after certain critical liquid times: Armco steel after 1868 s (a), S103 steel after 578 s (b), CK60 steel after 308 s (c) EN1.4034 steel after 338 s (d).

6.5b. Reasons for cracking

Based on the experimental results, it was proven that the primary reason for the cracking is the formation of MnS / Mn(Cr)S sulfide phases, which form in the joint during cooling, (see Fig.C10). The MnS / Mn(Cr)S phases are not present in the joint prior to the experiment. Instead, they form in the copper joint as a result of dissolution and diffusion of Mn, Cr and S elements from the bulk of steel into the liquid copper at the experimental temperature.

The reasons of cracking the joint at the MnS/Cu interface are the following:

i) The molar volume of ionic MnS precipitating in the solid copper joint is lower than the sum of partial molar volumes of Mn and S dissolved in copper joint. This local volume decrease accompanying MnS precipitation acts as a crack initiator at the MnS/Cu interface in the joint.

ii) The MnS precipitate is ionic and it precipitates in metallic copper joint. During cooling, the ionic MnS precipitate and metallic Cu matrix contract differently owing to their significantly different thermal expansion coefficients leading to additional stress at the MnS/Cu interface.

iii) There is a weak adhesion energy at the interface of ionic MnS and metallic Cu due to van-der-Waals forces. Thus MnS/Cu interface is the most probable place to form a crack compared to other interfaces, which are all metal/metal interfaces, such as the Cu/steel interface.

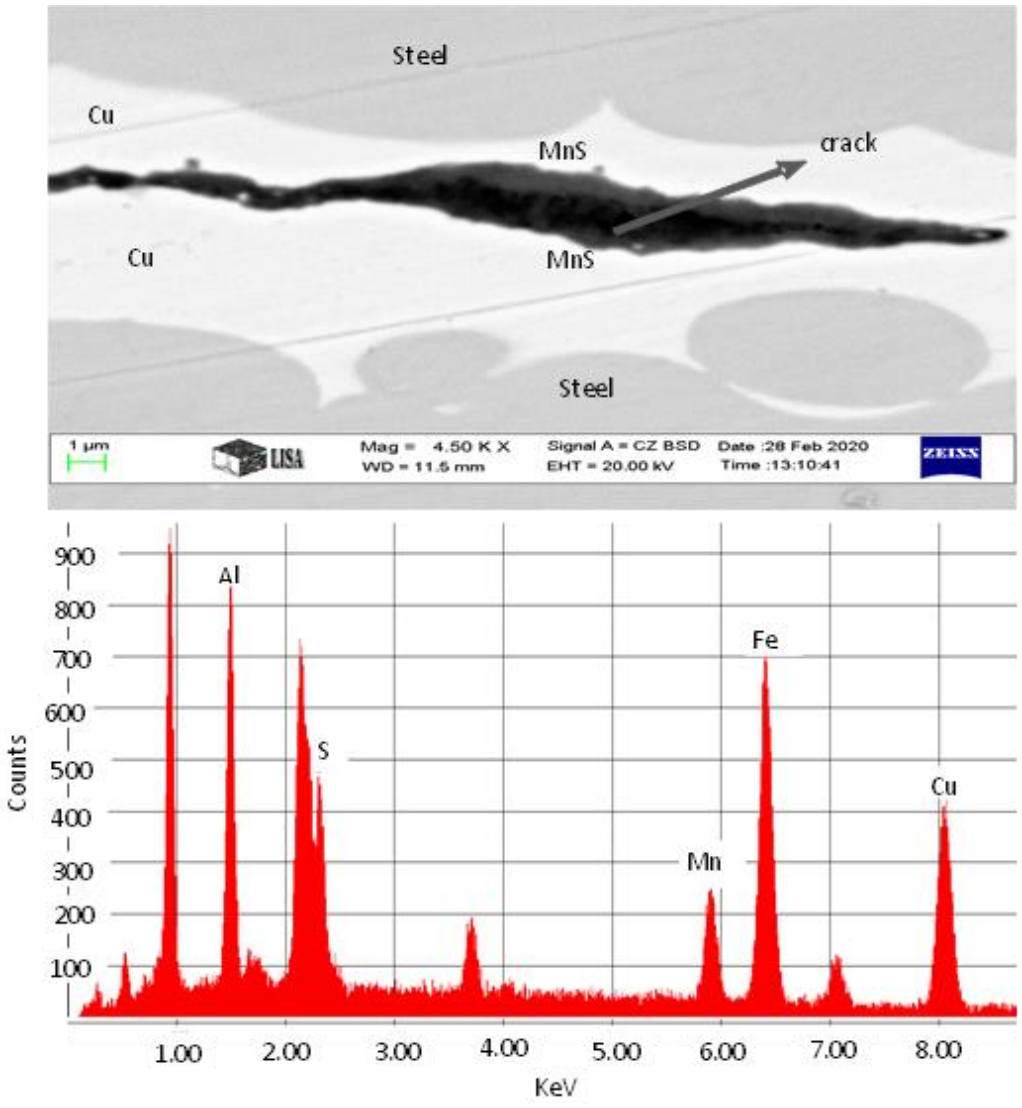

Fig.C10. The SEM image of the cross section of CK60 steel after 338 s liquid time of brazing experiment and the corresponding EDS spectra of the spot in the middle of the joint. We see Fe, Mn and S coming from steel while Cu being the joint. Additionally, we also observe Al which comes from polishing.

6.5c. Braze-integrity diagram

The results obtained above were summarized in the "braze-integrity" diagram. The graph shows the relation between liquid time and solubility product of MnS in the steel. The graph is divided into two technological regions separated by a demarcation line between cracked and crack-free joints (see Fig.C11). The demarcation line is given by Eq. (C3):

$$t_{L,cr} \cong \frac{151}{\sqrt[4]{c_{Mn(steel)} \cdot c_{S(steel)}}} \quad \text{(C3)}$$

with 151 ($s/\sqrt{w\%}$) and power of 4 (dimensionless) being semi-empirical parameters, valid for all steel types studied in this work.

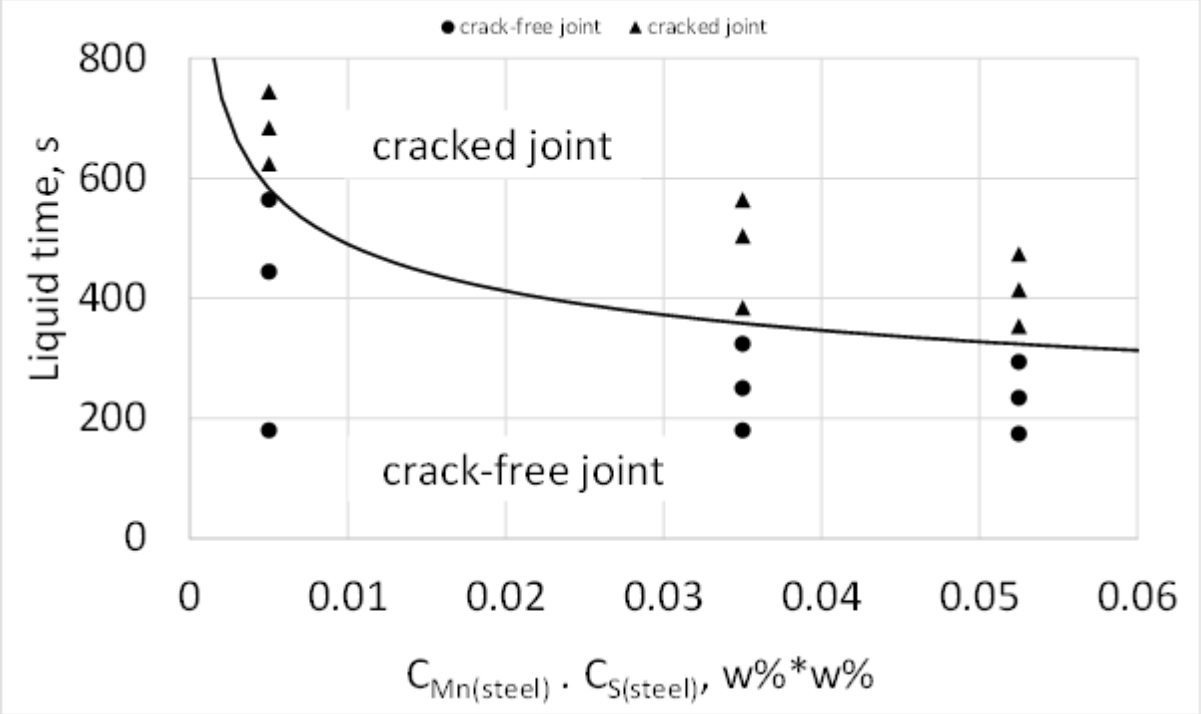

Fig.C11. The braze integrity diagram for Cu braze used for different steels with different Mn- and S-contents as function of liquid time.

7. Future possibilities

- Further experiments are needed on better understanding the pressure dependence on the non-wetting to wetting transition of the said metallic liquids. This would help in better control of pressure and temperature parameters during the joining applications like brazing in the industries.
- It would also be interesting from science point of view to observe experimentally the conditions under which the joint thinning effect (reported throughout my study) occurs in a brazed joint. For example, change in brazing atmosphere may reduce/increase the

joint thinning effect. Also, to observe if the composition of steels has any effect on the reduction of the joint thickness and extend the study to various steel grades.

8. Acknowledgements

I would like to thank “Antal Kerpely Doctoral School of Material Science and Technology” and Prof. Zoltan Gacsi, head of the doctoral school for providing me the opportunity to carry out PhD. My gratitude extends to the Institute of Physical Metallurgy, Metal Forming and Nanotechnology and Prof. Valeria Mertinger for providing me with all the necessary equipment for carrying out my research. I would like to thank Dr. Kovacs Arpad, Dr. Daniel Koncz-Horvath and Dr. Greta Gergely for extending their kind cooperation and scheduling of the SEM microstructural examination. I would also take the opportunity to show my gratitude to Dr. Anna Sycheva and Innovacios Laboratories for providing with SEM investigation of the samples. I would like to acknowledge the contributions of Bay-Zoltan non-profit kft and Mr. Jozsef T. Szabo for providing me with the experimental equipment in the initial phase of my PhD. A special thanks to Mrs. Aniko Markus and Mrs. Napsugar Bodnar for helping with both pre- and post-experimental sample preparation throughout the duration of my PhD. I would like to sincerely thank Mrs. Judit Szabo, Mrs. Agnes Solczi, Dr. Sveda Maria, Dr. Katalin Voith, Mrs. Nora Orosz-Forizs and Mrs. Stumpf Eva for their continued and valuable support in the administrative work at the university. My heartfelt gratitude for Tempus Public Foundation, Stipendium Hungaricum scholarship program and GINOP2.3.2-15-2016-00027 “Sustainable operation of the workshop of excellence for the research and development of crystalline and amorphous nanostructured materials” project implemented in the framework of the Szechenyi2020 program for financing the studies and providing the financial sustenance.

9. References

1. Kaptay, G. (2008). A unified model for the cohesive enthalpy, critical temperature, surface tension and volume thermal expansion coefficient of liquid metals of bcc, fcc and hcp crystals. *Materials Science and Engineering: A*, *495*(1-2), 19-26.
2. Kaptay, G. (2020). A coherent set of model equations for various surface and interface energies in systems with liquid and solid metals and alloys. *Advances in Colloid and Interface Science*, 102212.
3. Roberts, P. (2013). *Industrial brazing practice*. Crc Press.
4. Ishigami, I., Tsunasawa, E., & Yamanaka, K. (1981). Effects of vacuum heating conditions on the surface brightness of various stainless steels. *Transactions of the Japan Institute of Metals*, *22*(5), 337-346.
5. Arata, Y., Ohmori, A., & Cai, H. F. (1983). Studies on vacuum brazing (report II). *Transactions of IWR112*, *1*, 27-34
6. Kozlova, O., Voytovych, R., Devismes, M. F., & Eustathopoulos, N. (2008). Wetting and brazing of stainless steels by copper–silver eutectic. *Materials Science and Engineering: A*, *495*(1-2), 96-101.

7. Rousseau, A. F., Partridge, J. G., Gözükara, Y. M., Gulizia, S., & McCulloch, D. G. (2016). Carbon evolution during vacuum heat treatment of High-Speed Steel. *Vacuum*, *124*, 85-88.
8. Hawkins W D 1952 Physical Chemistry of Surface Films. Van Nostrand-Reinhold, New York
9. Young, T. (1805). III. An essay on the cohesion of fluids. *Philosophical transactions of the royal society of London*, (95), 65-87.
10. Naidich, Y. V., Perevertailo, V. M., & Obushchak, L. P. (1975). Contact properties of the phases participating in the crystallization of gold-silicon and gold-germanium melts. *Soviet Powder Metallurgy and Metal Ceramics*, *14*(7), 567-571.
11. Eustathopoulos, N., Nicholas, M. G., & Drevet, B. (Eds.). (1999). *Wettability at high temperatures*. Elsevier.
12. Naidich, J. V. (1981). The wettability of solids by liquid metals. In *Progress in surface and membrane science*,(14) 353-484. Academic Press, New York.
13. Ishida, T. (1988). Spreading kinetics of liquid metals on mild steel. *Materials science and technology*, *4*(9), 830-835.
14. McLean, D. Grain boundaries in metals'; 1957. *London, Oxford University Press.*
15. Lejcek, P. (2010). *Grain boundary segregation in metals* (Vol. 136). Springer.
16. Schmatz, D. J. (1983). Grain boundary penetration during brazing of aluminum. *Welding Journal*, *62*(10), 267-271.
17. Straumal, B. B., Gust, W., & Molodov, D. A. (1995). Wetting transition on grain boundaries in Al contacting with a Sn-rich melt. *Interface Science*, *3*(2), 127-132.
18. Y. S. Kwon, K. B. Gerasimov, S. S. Avramchuck, *Journal of Alloys and Compounds*, *359*(1-2), 79-83, (2003).
19. M. J. Assael, A. E. Kalyva, K. D. Antoniadis, R. Michael Banish, I. Egry, J. Wu, W. A. Wakeham, *Journal of Physical Chemistry Reference Data*, *39*(3), 033105, (2010).
20. Ishida, T. (1986). The interaction of molten copper with solid iron. Journal of materials science, 21(4), 1171-1179.
21. Fredriksson, H., Hansson, K., & Olsson, A. (2001). On the mechanism of liquid copper penetration into iron grain boundaries. Scandinavian journal of metallurgy, 30(1), 41-50.
22. Heiple, C., Bennett, W., & Rising, T. (1982). Embrittlement of several stainless steels by liquid copper and liquid braze alloys. *Materials Science and Engineering*, *52*(3), 277-289.
23. Nippes, E. F., & Ball, D. J. (1982). Copper-Contamination Cracking: Cracking Mechanism and Crack Inhibitors. *Welding Journal*, *61*(3), 75.
24. Maciejewski, J. (2005). Liquid metal induced embrittlement in fuel line braze joints. *Journal of Failure Analysis and Prevention*, *5*(2), 55-60.
25. Ghovanlou, M. K., Jahed, H., & Khajepour, A. (2011). Mechanical reliability characterization of low carbon steel brazed joints with copper filler metal. *Materials Science and Engineering: A*, *528*(19-20), 6146-6156.
26. Temmel, C., Karlsson, B., & Ingesten, N. G. (2008). Fatigue crack initiation in hardened medium carbon steel due to manganese sulphide inclusion clusters. *Fatigue & Fracture of Engineering Materials & Structures*, *31*(6), 466-477.

27. Mortensen, A., Drevet, B., & Eustathopoulos, N. (1997). Kinetics of diffusion-limited spreading of sessile drops in reactive wetting. *Scripta Materialia*, *36*(ARTICLE), 645.
28. Briant, C. L., & Banerji, S. K. (1978). Intergranular failure in steel: the role of grain-boundary composition. *International metals reviews*, *23*(1), 164-199.
29. Kameda, J., McMahon, C.J. The effects of Sb, Sn, and P on the strength of grain boundaries in a Ni-Cr Steel. *Metallurgical Material Transactions A* **12,** 31–37 (1981).
30. Kaptay, G. (2005). Modelling interfacial energies in metallic systems. In *Materials Science Forum*, 473, 1-10.

10. Notable Author publications in the subject of the thesis

10.1. Journal papers

J1: D.Varanasi, D.Koncz-Horvath, A.Sycheva, P.Baumli, G.Kaptay. Cracking of copper brazed steel joints due to precipitation of MnS upon cooling. J Mater Eng Perform (2020) doi:10.1007/s11665-020-05293-9. (2019-IF = 1.652, Q2 in 2019 in “Mater Sci (misc)”).

J2: Dheeraj Varanasi, Khaldun Emad Aldawoudi, Peter Baumli, Daniel Koncz-Horvath, George Kaptay, “Non-wetting to wetting transition temperatures of liquid tin on steel surfaces corresponding to their spontaneous deoxidation”, submitted to Archives of Metallurgy and Materials (Q3), under review.

J3: Varanasi, D., Szabo, J. T., & Baumli, P.: Investigation of the Copper Penetration and Joint Microstructure Observed in Low Alloyed Steels. NanoWorld J, 5(3) (2019), 36-40.

J4: Nuilek, K., Simon, A., Kurovics, E., Ibrahim, J. F. M., Varanasi, D., & Baumli, P. (2020, April). Effect of activation and exfoliation on the formation of carbon nanosheets derived from natural materials. In *Journal of Physics: Conference Series* (Vol. 1527, No. 1, p. 012036). IOP Publishing.